Oceanographic Data Retrieval with Tandem-L

Steffen Suchandt[1], Andrey Pleskachevsky[1], Daniela Borla Tridon[2]
[1]German Aerospace Center (DLR), Remote Sensing Technology Institute, Germany
[2]German Aerospace Center (DLR), Microwaves and Radar Institute, Germany

Abstract

Monitoring of the manifold dynamic processes on the Earth's surface is essential for characterizing and quantifying environmental changes and climate variability. Tandem-L has been proposed as a highly innovative L-band SAR satellite mission to provide observations and data products of unprecedented resolution, quality and revisit rates for the geosphere, biosphere, cryosphere and hydrosphere. In this paper we analyze the potential of Tandem-L for oceanographic applications.

1 Introduction

With Tandem-L, a SAR satellite mission for mapping dynamic processes in the Earth's biosphere, geosphere, cryosphere and hydrosphere has been proposed. For the flexible Tandem-L SAR instrument several advanced techniques like a large reflector antenna, digital beam forming (DBF), Scan-on-Receive (SCORE) as well as so called staggered SAR with variation of the pulse repetition interval for high-resolution and continuous wide-swath imaging will be implemented [1]. Tandem-L is driven by strong scientific interest in improved understanding and quantification of Earth system processes, which are relevant in many contexts such as climate variability, occurrence of natural disasters or sustainability. The mission aims at long-term monitoring of such processes on global scale, short revisit times, high resolution and unprecedented accuracy, thereby creating new data products. Main objectives are the global measurement of 3-D forest structure and biomass (biosphere), monitoring of Earth surface deformations (geosphere), measurement of glacier dynamics and melting (cryosphere) as well as high-resolution measurement of near-surface soil moisture changes and systematic mapping of coastal zones and sea ice (hydrosphere) [1][2].

In this paper we analyse the potential of Tandem-L for ocean monitoring, specifically, for retrieving information on surface currents, wind fields and sea state. Frequent measurements of such parameters are needed in different contexts. For instance, the feedback between the atmosphere and the deep ocean through the surface boundary layer plays an important role in climate regulation [3] and is influenced by the sea surface dynamics. Furthermore, surface currents are counted among the essential climate variables.

2 Observation of ocean regions

The potential for ocean observation is determined by the available imaging modes and by the overall observation strategy. Tandem-L data acquisition can be differentiated at top level after measurement modes: a 3-D structure mode (I) for fully-polarimetric mapping of e.g. height, structure and density of volume scatters by single-pass interferometry, a deformation mode (II) for monitoring small displacements of the Earth's surface by repeat-pass interferometry and additional high-resolution (wide swath) modes (III) for e.g. ocean monitoring or observation of natural disasters (floods, earthquakes etc.). These are based on various instrument modes and settings. The main parameters of the Tandem-L SAR sensors [2] are shown in **Table 1**. The observation concept covers alternating phases of modes (I) and (II) and an interspersed monitoring of selected (ocean) sites in other modes (III). All cases offer potential for frequent monostatic (single-channel) imaging of many ocean regions. In mode (I) bistatic interferometric data acquisition, with one sensor transmitting and both sensors receiving, is used over land areas. Bistatic acquisition is switched to monostatic, single-satellite operation after coastline crossing, to limit the high emerging data volume.

Instrument parameter	Value
Sensor height h	745 km
Sensor velocity v_s	7500 m/s
Radar wavelength λ	23.6 cm
Range bandwidth B_{rg}	$\leq$ 84 MHz
Polarization	single (S), dual (D), quad (Q)
Swath width s	$\leq$ 350 km @ S/D-pol
	$\leq$ 175 km @ Q-pol
PRF	2365 Hz
Azimuth resolution ρaz	7 m @ s $\leq$ 350 km, S/D-pol
	@ s $\leq$ 175 km, Q-pol
	1 m @ s $\leq$ 50 km, S/D/Q-pol
Incidence angle ϑ	26.3 - 47.0°
NESZ	< -25 dB

Table 1: Tandem-L main instrument parameters.

For some small selected areas, the bistatic acquisition can occasionally be extended to the ocean. In mode (II) data are acquired monostatically. For case (III) both mono- and bistatic data acquisition are used. While wind and sea state parameter can be retrieved with the same techniques likewise on mono- and bistatic data acquisitions, the method of surface current retrieval depends on the concrete mode (monostatic with one or two satellites, bistatic etc.).

2.1 Surface current measurement

In this section, we analyse techniques of surface current data retrieval for Tandem-L conditions. *Along-track interferometry (ATI)* uses the phase difference ϕ_{ATI} between two SAR images of the same area, acquired with a time lag Δt, to measure the cross-track component of the total surface current vector. The sensitivity to cross-track ground motion v_g is given by $\phi_{\mathrm{ATI}} = 4\pi/\lambda \cdot \Delta t \cdot v_g \cdot \sin\vartheta$ and $\Delta t = B_{\mathrm{ATI}}/v_s/i$, B_{ATI} being the spatial along-track baseline and $i = \{1 \mid \text{monostatic}, 2 \mid \text{bistatic}\}$. As the sea surface backscatter decorrelates after coherence time t_c, Δt must be shorter than this. For a fully developed sea, t_c can be estimated by

$$t_c = \frac{1.45 \cdot \lambda}{u} \left[\operatorname{erf}(2.69 \frac{\rho}{u^2}) \right]^{-1/2} \quad (1),$$

u being the wind speed, ρ the geometric mean of the effective, i.e. multi-looked interferogram range and azimuth resolutions on ground [4]. For example, azimuth and ground-range resolutions of ρ_{az} = 7 m by ρ_{grg} = 5.3 m, respectively (B_{rg}=40 MHz, ϑ=45°) and a multi-looking factor of 40 in each dimension of the ATI phase yielded $(244\ \mathrm{m})^2$ resolution of the derived surface velocity. For this, wind speeds of 5-15 m/s imply coherence times of 68 ms down to 23 ms, requiring B_{ATI} to be shorter than 1024 m down to 342 m in the bistatic (single-pass), or half of that in the monostatic (repeat-pass) case. It must be evaluated, where such along-track distances are available with the flown orbit configuration and acquisition strategy.

The achievable resolution of a surface velocity data product derived by ATI depends essentially on the temporal decorrelation γ_{temp} and on the SNR decorrelation γ_{SNR}. While γ_{temp} is governed by the ATI time lag and the coherence time, γ_{SNR} is influenced by the NESZ and the normalized radar cross section NRCS of the sea surface, the latter depending strongly on wind speed. A simulation for NESZ = -25dB, ϑ = 45°, an exemplary spatial resolution of 33 m x 33 m of the velocity data product (image resolutions as aforementioned and multi-looking L=30) and a wind speed of 10 m/s and using the L-band VV geophysical model function (GMF) developed in [5] to obtain the sea surface NRCS, shows that for these conditions a velocity accuracy < 0.15 m/s can be achieved at ATI baselines from approx. 200 – 600 m in the single-pass case (half of that in the repeat-pass case). This can, at the cost of losing spatial resolution, be further improved by choosing higher values for L.

Also, the influence of the cross-track baseline B_{XTI}, always being present and introducing a topographic phase component in the interferogram, has to be evaluated.

Alternatively, the cross-track component of the surface current can be obtained by *Doppler-centroid shift analysis (DCA)* on Tandem-L single-channel data. The method has successfully been demonstrated for various spaceborne SAR sensors including TanDEM-X [6]. It exploits the deviation of the Doppler centroid f_{DC} from its reference value $f_{DC,ref}$ as a function of the cross-track ground motion component by $f_{DC} - f_{DC,ref} = -2/\lambda \cdot v_g \cdot \sin\vartheta$. The achievable accuracy and resolution of surface velocities from DCA are comparable to the ones from ATI and depend on the accuracy of $f_{DC,ref}$, on the image resolution and on the window size used to estimate f_{DC}.

Tandem-L also enables to derive the total, i.e. 2-D sea surface velocity vector. Recently*, the maximum cross-correlation (MCC)* technique has been demonstrated for the TanDEM-X pursuit monostatic mode [7]. It is based on tracking similarities of the sea surface NRCS of two SAR images acquired with a time lag of several seconds in between. Hence, this method is suitable for Tandem-L acquisitions with larger along-track baselines in the order of tens of km. The minimum current speed that can be derived this way is determined by the image resolution and by the time lag.

More detailed results on the analysis of the achievable surface current data accuracy and resolution with respect to Tandem-L parameters are presented at the conference.

2.2 Wind data and sea state retrieval

Here, we look at the potential for the retrieval of meteo-marine parameters with Tandem-L. Various schemes to extract such data from (but not exclusively) L-band SAR have been developed.

Wind speed estimation is based on spatially averaged measurements of the normalized radar cross section [5][8]. Empirically derived GMF are used to relate local wind conditions and imaging geome-

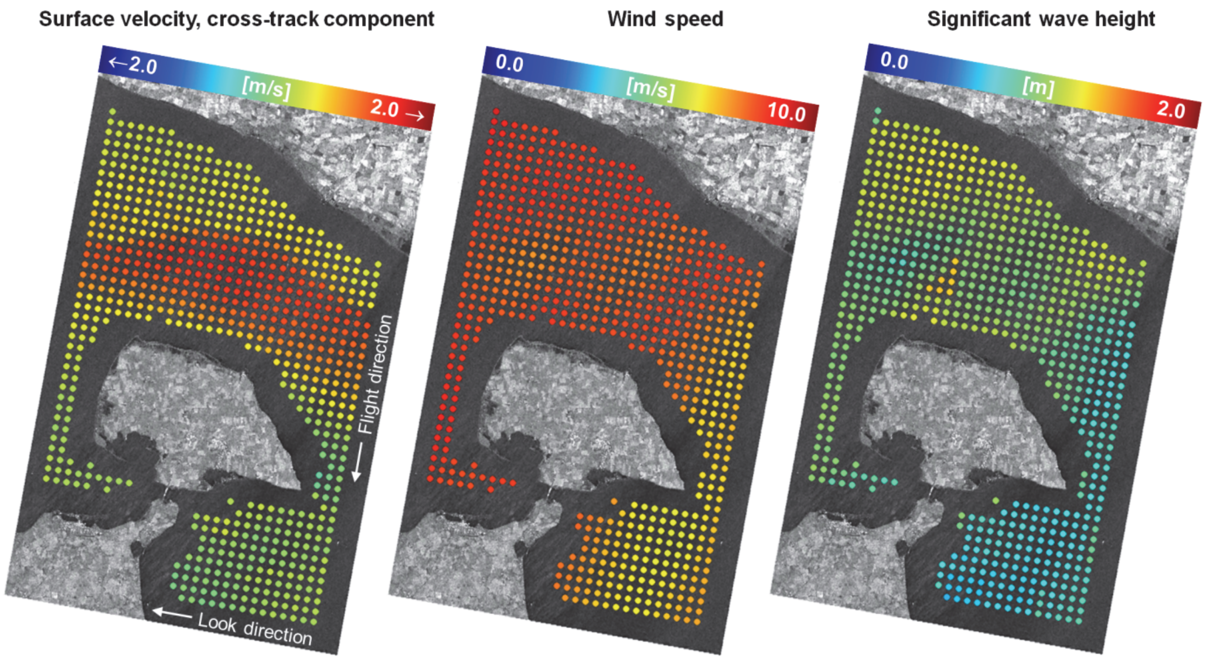

Figure 1: Demonstration of multiple ocean parameter retrieval from bistatic interferometric SAR satellite data (TanDEM-X) for the Fehmarn Belt, Germany, Jan. 30th, 2016: Surface velocity (cross-track component) extracted by ATI, wind speed from backscatter and significant wave height from image spectrum (left to right).

try to NRCS values. Since the NRCS characteristic depends on radar wavelength and polarization, the GMF needs be specific for it and even for the SAR sensor. A GMF for L-band, HH polarization, wind speeds of 0-20 m/s and incidence angles of 17°-43° has been derived for ALOS-PALSAR, admitting wind speed estimates of ~2 m/s accuracy [9]. In L-band, co-polarized, preferably VV data are best suited for wind speed retrieval, as they show significant higher NRCS over ocean than cross-polarized data [10]. The quality of the SAR-derived wind speed also depends on the noise level and the radiometric sensor calibration. For optimal results, thereby also regarding the ten-year mission lifetime, it is desirable to develop a Tandem-L specific GMF. This would be supported by an observation concept that, from the beginning, includes as many as possible ocean acquisitions in dual- (HH/VV) or single-pol (HH, VV), which also allow for a broad swath width and a large range of incidence angles (26.3°- 47.0°). The latter is obtainable probably at higher latitudes.

The estimation of sea state parameters like significant wave height H_s as well as of dominant wave period *DWP* and direction *DWD* from SAR exploits signal intensity modulation and evaluates the image spectrum of sub-scenes. This is done either by designing modulation transfer functions (MTF) for wave spectra, followed by integration and estimation of the parameters, or, by direct estimation from the image spectra using empirical functions as shown e.g. in [11] for L-band (ALOS/PALSAR). The often applied MTF approach usually involves high-resolution wind speed data, which, by the way, are also needed to correct measured surface velocities for wave motion. This highlights the importance of combined sea surface parameter retrieval from the same Tandem-L data acquisitions.

2.3 Demonstration with TanDEM-X

The great potential of Tandem-L for ocean monitoring and meteo-marine parameter retrieval can be demonstrated using the on-going TanDEM-X mission. **Figure 1** gives an example, in which different ocean parameters were extracted from the same TanDEM-X bistatic interferometric data. Using ATI, the cross-track component of the total surface velocity vector has been measured at gridded positions (left). The monostatic image of the co-registered SSC (CosSSC) pair was used in parallel to extract wind speeds and significant wave heights from the NRCS and from locally calculated wave spectra, respectively, for the same data grid [12]. The wind speed data were used for a local correction of the estimated surface velocity for wave contributions. In fact, combined ocean data products like this, regularly retrieved with Tandem-L, would be of high value for the ocean and environmental science communities.

3 Conclusions

The rapid development of the satellite techniques, SAR sensors, SAR processors, information extraction algorithms and ground infrastructures enabled a series of oceanographic applications during the last years, some even with near real-time (NRT) capability. Different kinds of data layers like wave parameters, surface wind speed and currents can be extracted in parallel from the same imagery. Beyond using them as separate data products, the different information layers can beneficially be combined to improve their quality. For example, the high-resolution SAR wind data can be used to correct the extracted surface velocities for wave motion. Furthermore, combining the data layers with additional information from the same acquisitions like ship detections supports maritime situation awareness (MSA) applications. The algorithms developed for these purposes for X- and C-band are integrated currently into prototype processors [13][14], which can be extended for Tandem-L.

References

[1] A. Moreira, G. Krieger, I. Hajnsek, K. Papthanassiou, M. Younis, P. Lopez-Dekker, S. Huber, M. Villano, M. Pardini, M. Eineder, F. de Zahn and A. Paruizzi, *Tandem-L: A Highly Innovative Bistatic SAR Mission for Monitoring Earth's Dynamic Processes*, IEEE Geoscience and Remote Sensing Magazine, vol. 3, issue 2, 2015.

[2] G. Krieger et al., Tandem-L: *Main Results of the Phase A Feasibility Study*, Proc. of IEEE IGARSS 2016, 10.-15. Jul. 2016, Bejing, China, pp. 2116-2119.

[3] N. Howe, *The impact of air-sea fluxes on the thermohaline circulation*, Royal Meteorological Society, Weather magazine, vol. 63, no. 8, Aug. 2008.

[4] M. J. Tucker, *The decorrelation time of microwave radar echoes from the sea surface*, *Int. J. Remote Sens.*, vol. 6, no. 7, pp. 1075–1089, May 1985.

[5] S. H. Yueh, S. Dinardo, A. Fore and F. Li, *Passive and active L-band microwave observations and modelling of ocean surface winds*, IEEE Trans. Geosci. Remote Sens., vol. 48, no. 8, pp. 3087-3100, 2010.

[6] R. Romeiser, H. Runge, S. Suchandt, R. Kahle, C. Rossi and P. S. Bell: *Quality Assessment of Surface Current Fields From TerraSAR-X and TanDEM-X Along-Track Interferometry and Doppler Centroid Analysis*, IEEE Trans. Geosci. Remote Sens., vol. 52, no. 5, pp. 2759 – 2772, 2013.

[7] Y. Ren, X.-M. Li, G. Gao and T. E. Busche, *Derivation of Sea Surface Tidal Current From Spaceborne SAR Constellation Data*, IEEE Trans. Geosci. Remote Sens., vol. 55, no. 6, pp. 3236 – 3247, 2017.

[8] J. F. Vesecky and R. H. Stewart, *The observation of ocean surface phenomena using imagery from the SEASAT synthetic aperture radar*, J. Geophys. Res., vol. 87, no. C5, pp. 3397–3430, 1982.

[9] O. Isoguchi and M. Shimada, *An L-band ocean geophysical model function derived from PALSAR*, IEEE Trans. Geosci. Remote Sens., vol. 47, no. 7, pp. 1925–1936, Jul. 2009.

[10] O. Isoguchi and M. Shimada, *Polarization dependence of L-band measurements over the ocean on surface wind at 23-25° incidence angles*, Proc. IEEE IGARSS, 7.-11. Jul. 2008, Boston, M.A., USA.

[11] O. Isoguchi and M. Shimada, *Extraction of ocean wave parameter by ALOS/PALSAR,* Proc. APSAR, 26.-30. Sep. 2011, Seoul, South Korea.

[12] A.L. Pleskachevsky, W. Rosenthal and S. Lehner, *Meteo-marine parameters for highly variable environment in coastal regions from satellite radar images*, ISPRS J. Photogramm. Remote Sens., vol. 119, pp. 464-484, Sep. 2016.

[13] E. Schwarz, D. Krause, M. Berg, H. Daedelow, and H. Maass, *Near Real Time Applications for Maritime Situational Awareness*, Int. Archives of the Photogrammetry, Remote Sensing & Spatial Information Sciences, vol. 40-7/W3, pp. 999-1003, 2015.

[14] S. Suchandt and H. Runge, *Ocean Surface Observations Using the TanDEM-X Satellite Formation*, IEEE J. Sel. Topics in App. Earth Observ. Remote Sens., vol. 8, issue 11, pp. 5096-5105, 2015.